

# Physicochemical Variation in Nanogold-Based Ayurved Medicine Suvarna Bhasma Produced by Various Manufacturers Lead to Different In Vivo Bioaccumulation Profiles

Snehasis Biswas, MTech<sup>1</sup>, Mukesh Chawda, BAMS<sup>2</sup>,  
Kapil Thakur, PhD<sup>2</sup>, Ramacharya Gudi, MD<sup>2</sup>,  
and Jayesh Bellare, PhD<sup>1,3</sup> 

## Abstract

*Suvarna Bhasma* (SB) is a gold particle-based medicine that is used in *Ayurved* to treat tuberculosis, arthritis and nervous diseases. Traditionally, the *Ayurved* preparation processes of SB do exist, but they are all long, tedious and involve several steps. Due to this, there is a possibility of bypassing the necessary *Ayurved* processes or non-adherence to all steps or use of synthetic gold particles. Our aim is to characterize 5 commercial SB preparations from 5 different manufacturers. A comparative physicochemical, pharmacokinetic (PK) and bioaccumulation study was carried out on all the 5 SB preparations. The general appearance such as color and texture of these 5 samples were different from each other. The size, shape and gold concentration (from 32-98 wt%) varied among all the 5 SBs. The accumulation of ionic gold in zebrafish and gold concentration profiles in rat blood were found to be significantly different for all the 5 SBs. Non-compartmental PK model obtained from the concentration-time profile showed significant differences in various PK parameters such as peak concentration ( $C_{max}$ ), half-life ( $t_{1/2}$ ) and terminal elimination slope ( $\lambda_z$ ) for all the 5 SB preparations. SB-B showed the highest  $C_{max}$  (8.55  $\mu\text{g/L}$ ), whereas SB-D showed the lowest  $C_{max}$  (4.66  $\mu\text{g/L}$ ). The dissolution of ionic gold from SBs in zebrafish tissue after the oral dose had a 5.5-fold difference between the highest and lowest ionic gold concentrations. All the 5 samples showed distinct physicochemical and biological properties. Based on characteristic microscopic morphology, it was found that 2 preparations among them were suspected of being manufactured by non-adherence to the mentioned *Ayurved* references.

## Keywords

gold nanoparticles, Suvarna Bhasma, Ayurved, bioaccumulation, pharmacokinetics

Received October 13, 2020. Received revised February 2, 2021. Accepted for publication March 27, 2021.

## Introduction

Gold is one of the most attractive metals in human history having diverse applications in commercial uses as well as medicinal fields.<sup>1,2</sup> Gold has played an important role as a therapeutic agent in many ancient civilizations such as Egyptian, Chinese and Indian civilizations.<sup>3</sup> In modern medicine, gold nanoparticles find significant roles in biomedical applications such as drug delivery, diagnosis, biomedical imaging and many other applications.<sup>4,5</sup> *Suvarna Bhasma* (also known as *Swarna Bhasma*, SB) is a traditional *Ayurved* medicine that contains nano and colloidal gold particles and has been used in India for centuries to treat rheumatoid arthritis, diabetes and nervous system related diseases.<sup>6,7</sup> Owing to the presence of gold

nanoparticles in SB, research interest in SB has been renewed considering that it may have applications in biomedical uses of

<sup>1</sup> Department of Chemical Engineering, Indian Institute of Technology Bombay, Powai, Mumbai, Maharashtra, India

<sup>2</sup> Shree Dhootapapeshwar Limited, Nanubhai Desai Road, Khetwadi, Mumbai, Maharashtra, India

<sup>3</sup> Wadhvani Research Centre for Bioengineering, Indian Institute of Technology Bombay, Powai, Mumbai, Maharashtra, India

### Corresponding Author:

Jayesh Bellare, Department of Chemical Engineering, Indian Institute of Technology Bombay, Powai, Mumbai 400076, Maharashtra, India.  
Email: jb@iitb.ac.in



**Table 1.** SB From Various Manufacturers and Its Textual Manufacturing Reference.

Suvarna bhasma (sample code)	Manufacturing date	Textual manufacturing reference as per label	Batch no.
SB-A	03/2017	Siddh Yog Sangraha	16146002
SB-B	03/2018	Bharat Bhaishajya Ratnakar 5/8357	PI80300114
SB-C	11/2016	Sharangadhara Madhaymkhanda Ch.II	EK0019
SB-D	03/2017	Rasa Tarangini/panchadashastaranga	SB0220
SB-E	04/2018	Bharat Bhaishajya Ratnakar 8362	003

gold nanoparticles. Traditionally, SB is believed to enhance immunity and it also has antioxidant and anti-aging effects.<sup>8</sup>

SB is one of the most expensive medicines in *Ayurved* because it contains up to 98% gold. In India, it is manufactured by several large-scale manufacturers and numerous individual *Ayurved* practitioners. The rigorous and tedious *Ayurved* manufacturing steps further add to the cost of SB. The renowned large-scale manufacturers of SB in India include Shree Baidyanath Ayurved Bhawan Pvt. Ltd., Dabur India Ltd., Shree Dhootapapeshwar Limited, Unjha Pharmaceuticals Pvt. Ltd. and Emami Limited. The manufacturing process of SB for different manufacturers may differ as per the textual method followed. The market price of SB varies from Rs 5000 (~\$ 70) to Rs 8000 (~\$ 115) for 1 g. SB was previously characterized by several research groups. However, the physicochemical properties reported in each article were different from others. For example, Beaudet et al,<sup>9</sup> Brown et al<sup>10</sup> and Thakur et al<sup>11</sup> reported gold concentration in SB as 57%, 92% and 98% respectively. This irregularity in results lead us to find out the reason behind the alteration in the physicochemical properties. Therefore, a comprehensive physicochemical characterization of SB manufactured by 5 major *Ayurved* companies was carried out.

Moreover, the *Ayurved* manufacturing process is lengthy and can produce only a limited quantity of SB at a time. Therefore, there is a possibility that some manufacturers may bypass the textual *Ayurved* process by eliminating some of the steps or by replacing them with more straightforward and cost-effective direct synthesis processes like chemical or electrochemical synthesis. SB has been used for centuries in humans and its efficacy and safety is well established. However, chemically synthesized gold particles cannot be termed as SB since they may not be therapeutically useful as SB as the size, shape, chemical composition and possibility of trace contamination can affect the biological interactions.<sup>12</sup> In this study, we characterized 5 marketed samples from the 5 different key manufacturers of SB. A comparative study was carried out concerning their morphology, chemical composition and contamination of heavy metals. From the physicochemical perspective, we tried to investigate whether the manufacturers followed any direct synthesis method for gold particles.

*Bhasma* particles, once they get into the body through oral administration, could be available in the blood circulatory system and can accumulate in various tissues. The pharmacokinetics profile in the body of *Bhasma* particles ingested organism may vary due to the variation in particle size and

shape. Therefore, the concentration profile of gold in blood with time was examined in the rat model after administration of similar amounts of doses of all the SB preparations so as to determine the difference in the amount delivered. Gold is not an essential metal for the biological system.<sup>13</sup> Gold particles are non-toxic, although ionic gold released from gold particles in the biological system may cause toxicity.<sup>14</sup> Therefore, it is also crucial to check whether the ionic gold released by these medicines is below the toxic level. Hence, the zebrafish model was employed in order to check the accumulation of soluble ionic gold released from SB in whole-body tissue after an oral dose.

## Materials and Methods

### Chemicals

All the 5 SB preparations from different manufacturers were purchased from the authorized *Ayurved* shops/outlets. After purchasing the SB preparations, the labels of respective preparations were removed and replaced with random code names such as SB-A, SB-B, SB-C, SB-D and SB-E, and thus blinded from analytical lab personnel. The code names and the textual references of SB manufacturing processes are enlisted in the following Table 1

### Manufacturing Process of Suvarna Bhasmas as per Textual Reference

In this study, all SB preparations were purchased. The details of the manufacturing processes have been included in the Supplementary file 1. Here, a representative flowchart is given for one of the SB manufacturing process described in *Ayurved* (Figure 1).

### Physicochemical Characterization of SB Samples

SB samples procured from the market were in the form of powder. The size, shape, crystalline phase and composition were analyzed utilizing various analytical techniques as follows:

The crystal phase of SB particles was identified by X-ray powder diffraction (XRD, Smart Lab, Rigaku, Japan). The diffraction pattern of SB was recorded using CuK $\alpha$  having a wavelength of 1.5406 Å. Observed XRD peak positions and intensities were matched to the International Centre for Diffraction Data (ICDD) to identify the possible phases present in the samples. The crystal size of SB samples was calculated using the Scherrer's equation. The thermal degradation property of SB particles was carried out using thermogravimetric analyzer (TGA, Perkin Elmer, USA) up to a temperature of 1350°C.

Particle size and shape were analyzed by transmission electron microscopy (TEM, JEOL 2100) and field emission gun—scanning

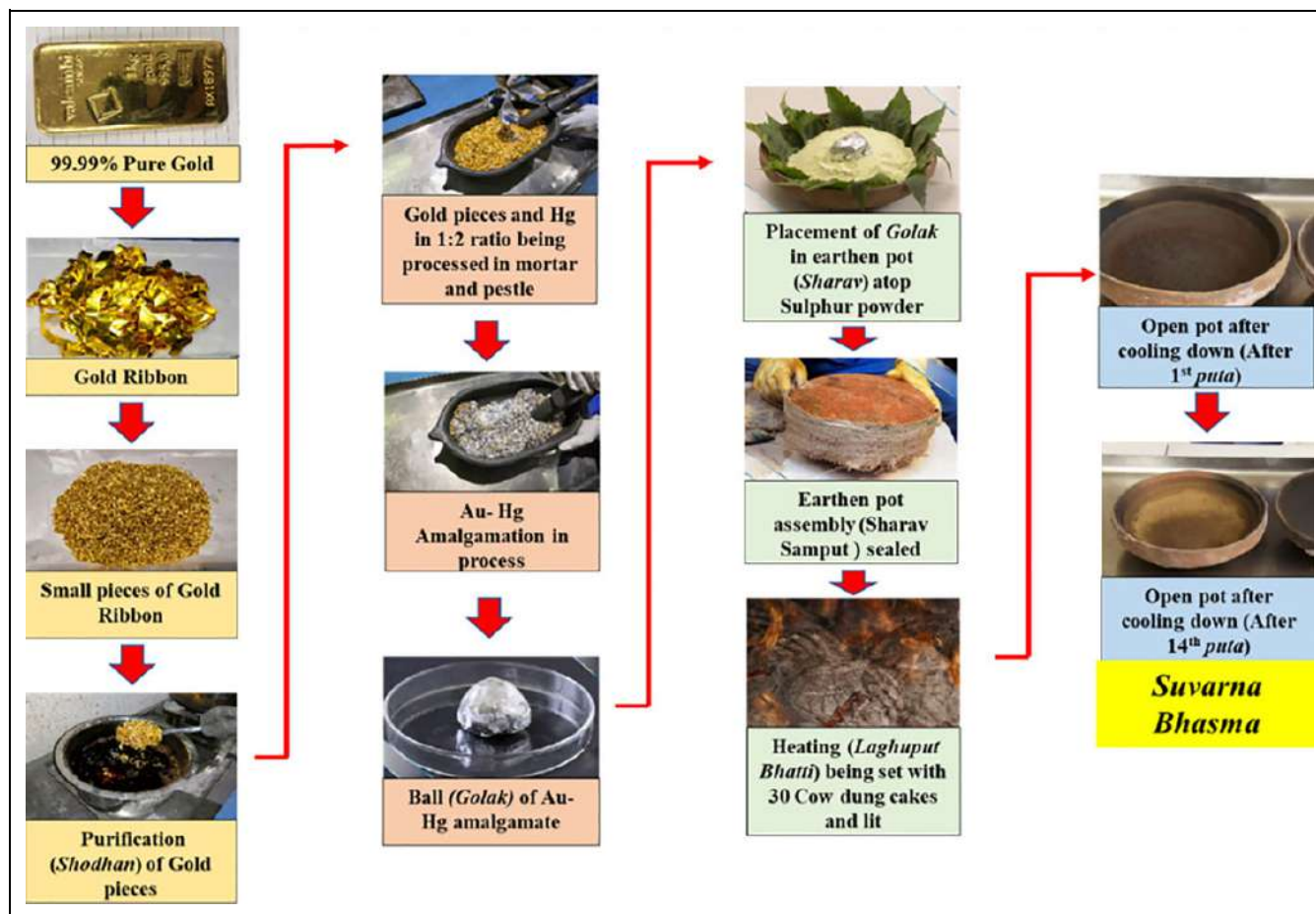


**Figure 1.** A representative schematic diagram of one of several ways of SB preparation. The heat treatment of gold-mercury amalgamate was carried out up to 750 °C along with sulfur powder. Each heat cycle (*puta*) required 10-14 h, and total time of SB may take up to 21 days. Although, preparation steps and ingredients vary from different manufacturers to manufacturers.

electron microscopy (FEG-SEM, JEOL JSM-7600F). The sample preparation for TEM was carried out by suspending SB samples in Milli-Q water and sonicated for 10 minutes. The suspended particles from the upper level of water were pulled out and kept on a carbon-coated copper grid separately and dried before analysis. Samples for SEM analysis were prepared by fixing SB samples on carbon tape. The surface area of SB particles was analyzed using a BET surface analyzer (3Flex, Micromeritics, USA).

Elemental analysis was carried out with energy-dispersive X-ray spectroscopy (EDS, Oxford instrument) attached with SEM and inductively coupled plasma atomic emission spectroscopy (ICP-AES, ARCOS, SPECTRO Analytical Instrument, Germany). For ICP-AES analysis, the samples ( $0.010 \pm 0.002$  g) were first digested in *aqua regia* (1:3 HNO<sub>3</sub>: HCl), then diluted with MilliQ water and subjected to analysis by ICP-AES. Pure gold samples (99.9%) were also digested in *aqua regia* similarly and provided as a reference standard for ICP-AES analysis. ICP-AES results of SBs were compared with reference pure gold standard.

### Animal Ethics

Animal experiments were conducted according to the Committee for the Purpose of Control and Supervision of Experiments on Animals (CPCSEA) guidelines (SDARF/CT/2019/04), India.

### Bioavailability of Gold in Rat Blood

A total of 20 Wistar rats of either sex with an average body weight of  $250 \pm 20$  g were divided into 5 groups ( $n = 4/\text{group}$ ). All the animals were fasted for 2 hours before dosing (feed of animals withheld, although animals were allowed to access water). Each rat from the respective group was dosed once with 0.8 mg/kg of respective SB preparations. Animals in all groups were administered SB mixed in cow ghee orally. After acclimatization, blood samples from all animals were collected at 0 hour, 6 hours, 12 hours, 24 hours, and 48 hours after administration of SB. Feed was offered to animals after 2 hours post SB administration.

Estimation of gold content of blood was carried out using ICP-OES (Inductively coupled plasma-optical emission spectrometry, Perkin Elmer, Model-Avio 200). Quickly, 1.5 ml of whole blood was collected aseptically from animals in sterile EDTA vacutainer. Then blood was then transferred to the crucible for ash formation. To these ash samples, *aqua regia* (HNO<sub>3</sub>: HCL in ratio 1:3) was added. The mixture was kept for digestion at 60°C for 2 hours. After digestion, the mixture was filtered. The filtered sample was further used for the assay of gold content by ICP-OES. The National Institute of Standards and Technology (NIST) traceable gold was used as the reference standard.

The non-compartmental model was used to determine the pharmacokinetic parameters. The trapezoidal method was employed to

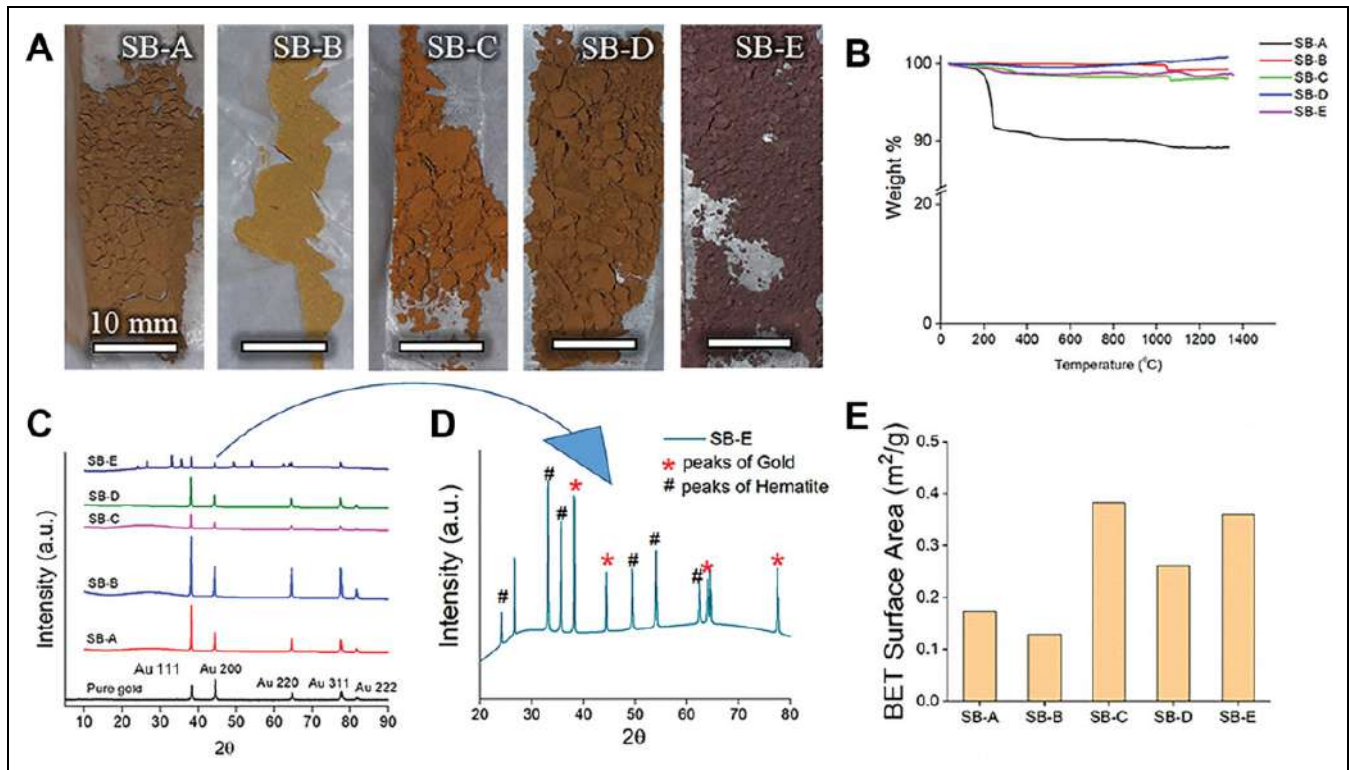


**Figure 2.** (A) The appearance of 5 marketed SB samples. (B) TGA, (C) XRD, (D) XRD of SBE, (E) BET surface area. Color of 5 samples differ from each other. TGA shows weight loss was highest for SB-A samples and lowest for SB-D and SB-B samples. The XRD peaks were compared with pure gold samples. All samples consisted of only face-centered gold crystalline phase, SB-E had additional peaks of iron oxides. Approximately 8% mass loss up to 210°C for samples SB-A.

investigate the area under the concentration-time curves from time 0 to time  $t$ . Peak concentration ( $C_{max}$ ) was found directly from the respective concentration-time curves. PKSolver<sup>15</sup> was used to calculate various PK parameters such as time of peak concentration ( $T_{max}$ ), terminal elimination slope ( $\lambda_z$ ), area under the zero and first-moment curves from 0 to last time  $t$  ( $AUC_{0-t}$ ,  $AUMC_{0-t}$ ), half-life ( $t_{1/2}$ ), mean residence time (MRT) and apparent volume of distribution based on the terminal slope ( $V_z/F$ ). The data obtained from the pharmacokinetic model were analyzed to find out statistical differences using Origin software. Significance alteration was examined using a 1-way analysis of variance (ANOVA) technique and found significant, if  $*p < 0.05$  after Fisher's least significant difference test (LSD). All the values are represented as mean  $\pm$  SEM.

### Accumulation of Ionic Gold in Zebrafish Tissues

Housing and caring of zebrafish were carried out as per our previous work.<sup>16</sup> Briefly, after 30 days of the acclimatization period in the zebrafish housing facility, the fish were divided into 5 groups for the 5 SB samples. Each group contained a cohort of 2 fish. Fish were administered SBs orally by mixing with their diet. The diet was prepared by mixing SB with fish food, and COD oil was used as a sticking substance. The diet was then analyzed by ICP-AES to evaluate the exact concentration of SB. A calculated amount of SB dose (0.1 mg/g body weight of fish) was given orally to the fish. After the drug administration, fish were euthanized, 24 hours after the single dose and digested in nitric acid (Supra pure, Merck). Nitric acid was used as it cannot digest gold particles and only the ionic gold released from the

SBs can be evaluated by inductively coupled plasma-mass spectroscopy (ICP-MS). A pool of 2 fish was considered as one for the respective SB treatment group. The experiment was quadruplicated.

## Results

### General Appearance

Figure 2A shows the difference in the color of the 5 SB preparations. The color of the SB-B was golden yellow, whereas SB-E was dark maroon. On the other hand, for SB-A, SB-C and SB-D, the colors were of different shades of chocolate color. The solubility of these 5 samples was checked in *aqua regia*, and except sample SB-E, all other 4 samples were completely soluble. Sample SB-E was partially soluble, which produced reddish residue in *aqua regia*, probably of iron oxide (confirmed later by XRD and ICP-AES).

### TGA Analysis

The TGA analysis (Figure 2B) showed that for sample SB-B and SB-D, loss in mass was negligible up to 1045 °C (<0.5%), whereas, for sample SB-E and SB-C, the weight loss was 1% and 1.5% respectively. The mass loss was highest for sample SB-A, which lost approximately 8% mass up to 250 °C and 11% up to 1045 °C. The mass loss of SB-A indicated the

**Table 2.** Crystallites Size of SB From Different Manufacturers.

Sample	Peak position (2-theta, deg)	FWHM (2-theta, deg)	Crystal size in nm (avg $\pm$ SEM)
SB-A	38.18	0.2166	39.87
	38.15	0.2037	$\pm$ 0.91
	38.14	0.2190	
SB-B	38.15	0.2173	40.32
	38.16	0.1850	$\pm$ 2.91
	38.09	0.2356	
SB-C	38.08	0.2527	37.58
	38.00	0.2236	$\pm$ 2.21
	38.09	0.2060	
SB-D	38.06	0.2016	40.73
	38.15	0.2160	$\pm$ 0.81
	38.18	0.2080	
SB-E	38.16	0.1035	77.89
	38.19	0.0900	$\pm$ 10.86
	38.13	0.1480	

presence of other composite materials, having low degradation temperature, along with gold.

### Crystallographic Analysis by XRD

XRD peaks of SB-A, SB-B, SB-C and SB-D were similar and exactly matched with pure gold (face-centered cube crystal structure, Figure 2C). However, the XRD of sample SB-E contained extra peaks along with gold peaks. The extra peaks in sample SB-E indicated the presence of other crystalline phases along with gold, possibly iron oxides (Figure 2D). The crystallites size of the samples was measured using Scherrer's equation from the most intense gold peak ( $hkl = 111$ ) and are represented in Table 2. The crystallites size was maximum for SB-E (77 nm), whereas, the other 4 samples had approximately similar crystallites size ( $\sim 40$  nm).

### BET Surface Area

BET surface area of SB-C sample was highest ( $0.38\text{m}^2/\text{g}$ ), whereas SB-B showed the lowest surface area (Figure 2E).

### TEM and SEM Backscatter Imaging

TEM and SEM images (Figure 3) showed that the morphology of all 5 SB preparations was different from each other. The maximum size of SB-B particles was highest as compared to other samples, up to  $60\ \mu\text{m}$  of gold particles were observed in SB-B (Figure 3B). The maximum size of particles observed was in the following order SB-B > SB-E > SB-C > SB-D > SB-A. From the TEM and SEM images, it could be illustrated that the shape of particles drastically varied from each other. The shape of SB-A (Figure 3A) and SB-B (Figure 3B) was irregular and of varying sizes. In these 2 preparations, it was observed that along with gold particles, other composites were attached to the crevices of those particles (grey in color in SEM images, Supplementary file 1, Figure S1). The shape of SB-C

was more homogeneous compared to the previous 2 samples (Figure 3C). The outer shape of most of the particles was elliptical or spherical for SB-C with a large number of internal crevices in the structure. Sample SB-D was the most uniform in size and shape among all samples; most of the particles were exactly spherical (Figure 3D). The shape of SB-E was irregular and a chunk of flake-like particles was associated with large particles (Figure 3E).

### EDAX Mapping

EDAX mapping of SB preparations revealed some interesting facts about these samples (Figure 4). In sample SB-A, a substantial amount of arsenic was found, whereas, sample SB-B, SB-C and SB-D contained minor elements like Fe, Ca, Na, O, P, etc. In sample SB-E, the abundance of gold was minimum; interestingly some big particles of SB-E did not even contain gold (Supplementary file 1, Figure S2).

### ICP-AES

Elemental analysis of SBs is represented in Table 3, which indicates variation in gold concentration as well as the concentration of other trace elements. Samples SB-B, SB-C and SB-D had the highest concentration of gold (95-98 wt.%); sample SB-A contained approximately 85% gold, whereas sample SB-E contained the least amount of gold (32-37 wt.%) when compared to other samples. Sample SB-A contained 5.4 wt.% of arsenic, whereas the other 4 samples did not show any arsenic content. Fe, Ca and Si were common in all samples. Sample SB-E had the highest concentration of Fe (19.5 wt.%) followed by SB-A (0.91 wt.%). Other 3 samples had 0.15-0.26 wt.% of Fe. Interestingly, despite using Hg in the processing steps, we did not find any Hg in any of the SB samples (was below detectable limit).

### Unique Morphological Features Found in the Marketed SB Samples

The microstructure of all SB samples possessed some unique morphology, which was detected either by SEM or TEM analysis (Figure 5).

*Sample SB-A:* The size and shape of sample SB-A were irregular. Some of the gold particles (in micron size) were coated with C, Si, Fe, O and As (Figure 5A).

*Sample SB-B:* This SB (SB-B) contained nano-sized, spherical gold particles that were coated with Na, Si, P and Fe (Figure 5B).

*Sample SB-C:* The microstructure of this sample was coral shaped, having porous structures (Figure 5C).

*Sample SB-D:* In sample SB-D, most of the particles were spherical with various sizes. The surface of the spherical particles was rough (Figure 5D).

*Sample SB-E:* Sample SB-E contained flake and rod-like structures embedded on large particles (Figure 5E).

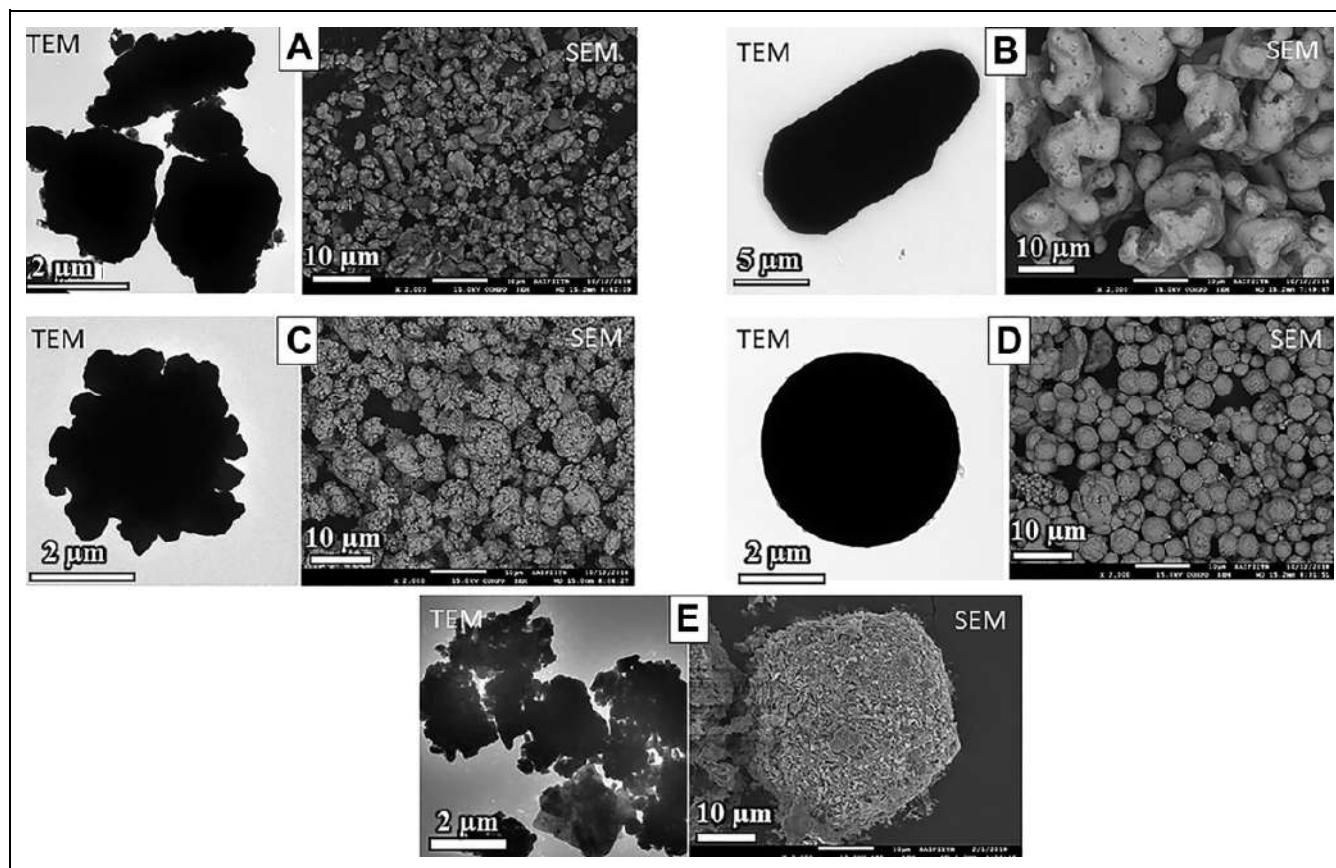


**Figure 3.** SEM and TEM images of SB samples. (A) SB-A, (B) SB-B, (C) SB-C, (D) SB-D, and (E) SB-E. Left-sided images are TEM images, whereas right-sided images are SEM images for every sample. Morphology of each sample was unique and different from each other. Most of the particles in SB-D was exactly spherical in shape.

### Bioavailability of Gold in Rat Blood

The schematic of the rat experiment is demonstrated in Figure 6A. Gold bioavailability in blood was established by measuring the time-dependent content of gold in the blood (Figure 6B). The concentration-time profile of SB-E was largely distinct from the other 4 samples, as it showed  $T_{max}$  at 10 hours, whereas other SB groups showed  $T_{max}$  at 24 hours after drug administration. The non-compartmental pharmacokinetic model (Table 4) showed a significant difference in  $\lambda_z$ ,  $T_{max}$ ,  $C_{max}$ ,  $AUC_{0-t_3}$  and  $V_z/F_{obs}$  parameters between various SB groups. SB-B showed the highest  $C_{max}$  gold concentration after 24 hours of drug administration among all the SB samples and SB-D showed the lowest. The  $C_{max}$  concentration was  $\sim 0.06\%$  of the total oral dose in blood for SB-B (considering blood volume of rat = 15 ml for 250 g body weight<sup>17</sup>).

### Accumulation of Ionic Au in Whole-Body Zebrafish Tissue

The accumulation of ionic gold released from the SB particles in zebrafish tissue was highest for SB-C samples, whereas for SB-E samples, it was the lowest (Figure 6C). In this case, we could see that the ionic gold (IG) released from SB depended on 2 factors—mainly surface area ( $A_i$ ) of gold particles and gold concentration ( $C_i$ ) in SBs. The plot between ionic gold

concentration and the product of  $A_i \times C_i$  (Table 5) is shown in the following figure (Figure 6D), which shows an excellent regressive linear fitting with  $R^2 = 0.974$ .

### Discussion

Many consider *Ayurved* as one of the most holistic and personal medicinal approaches, which is now gaining considerable acceptance worldwide. However, some concern is being raised against *Ayurved* medicines, especially for metal-based *Bhasma* medicines. Some researchers found heavy metals like Hg, Pb and As in *Ayurved* medicines in very high concentrations,<sup>18</sup> although *Ayurved* never denies the presence of heavy metal in its medicines since these are essential ingredients of these medicines. In *Ayurved*, the therapeutic uses of these metal-based medicines are restricted to specific diseases and the therapeutic dose is limited, since an overdose may cause toxicity instead of efficacy as per the *Ayurved* texts.

Unlike modern medicine, the *Bhasma* manufacturing process is not straight forward; inconsistency in physicochemical properties may occur between manufacturers as they follow different traditional manufacturing techniques for the *Bhasma* preparation.<sup>19</sup> Therefore, performing physicochemical characterization is of utmost importance to control the quality of these

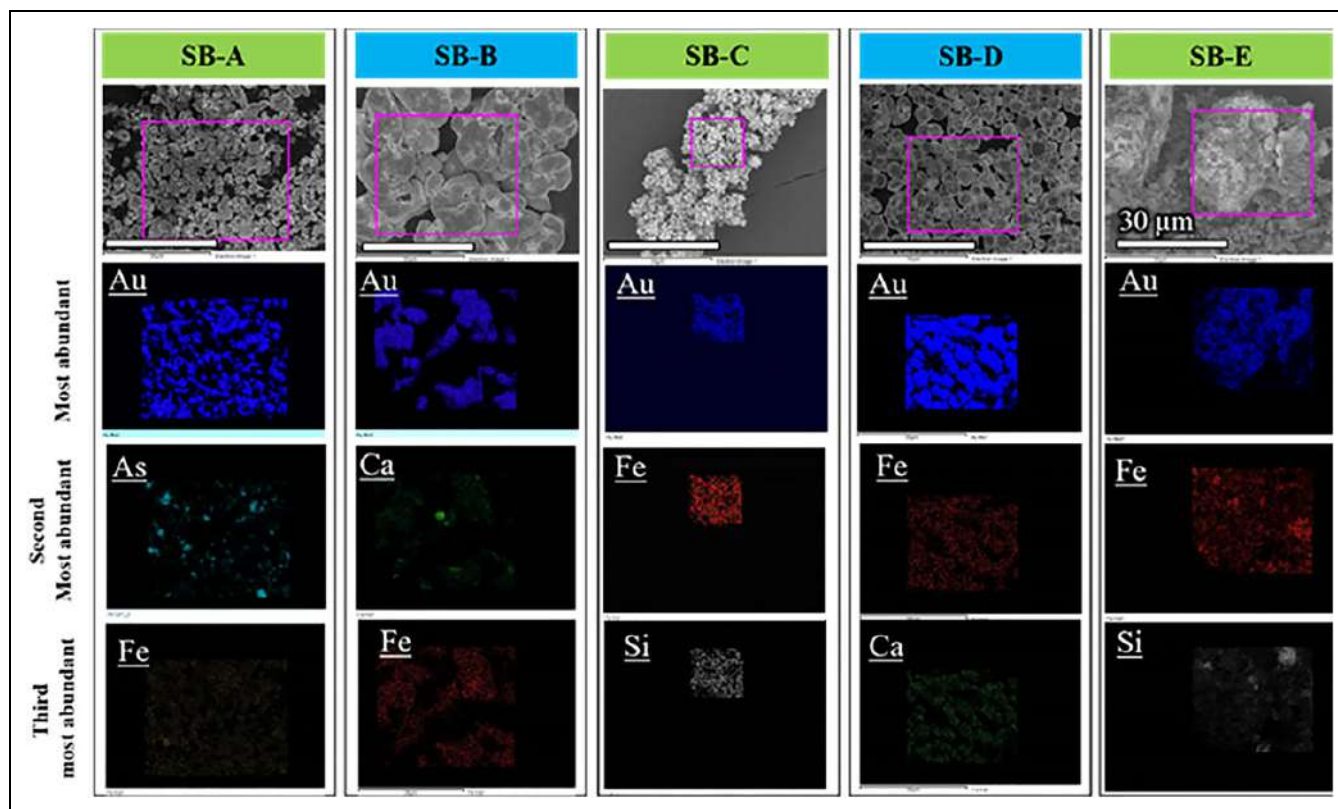


**Figure 4.** EDAX mapping of SB samples. Sample SB-A contained a considerable amount of arsenic. (Scale bar = 30 µm).

**Table 3.** ICP-AES Elemental Analysis of SBs (wt. %).

Elements	SB-A	SB-B	SB-C	SB-D	SB-E
Au	84-87	96-98	95-98	96-98	32-37
Hg	ND	ND	ND	ND	ND
S	ND	ND	ND	ND	ND
Si	1.36	0.77	0.31	0.67	0.91
As	5.4	ND	ND	ND	ND
Fe	0.91	0.15	0.18	0.26	19.5*
Pb	ND	ND	ND	ND	ND
Na	ND	0.08	ND	ND	ND
Ca	1.48	1	1.07	1.09	1.92

\*The total concentration of Fe in SB-E would be higher as SB-E is not completely soluble in aqua regia. ND = not detected.

traditional medicines. Otherwise, scientific validation of its efficacy is not possible as physicochemical properties of particles control their dynamic interaction with bodily fluids, cellular organelles and biomolecules<sup>12</sup> and hence, their efficiency.

Additionally, to bypass the lengthy *Ayurved* manufacturing process of SB (which may take 21 days), some manufacturers may choose to follow direct chemical or electrochemical methods, which could be another serious problem for its use in therapy. SB manufactured strictly as per the textual reference has a long history of human use that ensures both safety and efficacy. In *Ayurved* text, the dose limit and possible ill effects due to inappropriate administration of SB are well documented.

However, the modern synthesized colloidal particles have not been clinically validated for *Ayurved* use, and they may not be that efficient as SB. On the contrary, they could possibly have ill effects. Therefore, for SB production, these modern syntheses process should be avoided as they may not deliver the desired efficacy and safety, but more importantly, as they do not follow the accepted *Ayurved* pharmacopoeial texts.

Our results found enormous variations in physicochemical properties between different marketed SB preparations. First of all, the general appearance in terms of color varied for all SBs; this can happen due to compositional variation, particle size, duration of heat treatment, etc. In the case of SB-E, the brownish color was due to the presence of a high amount of iron oxides. Moreover, the morphology of all 5 preparations was different. The shape of SB-A was irregular and the average particle size was lower as compared to other preparations. The particles of SB-B were bigger as compared to other preparations and had crevices. In the crevices, coated spherical gold nanoparticles were observed. SB-C had coral shaped microstructure. SB-D sample had the most uniform spherical particles with an uneven surface, whereas, SB-E consisted of irregular big particles, which were attached with flake-like particles. The flake-like particles were not gold but a compound of Si, Ca, Fe, etc. Also, the concentration of gold differed among these SB preparations. The abundance of gold was minimum for SB-E. In SB-A, a significant concentration of arsenic (~5%) was found, whereas the remaining samples did

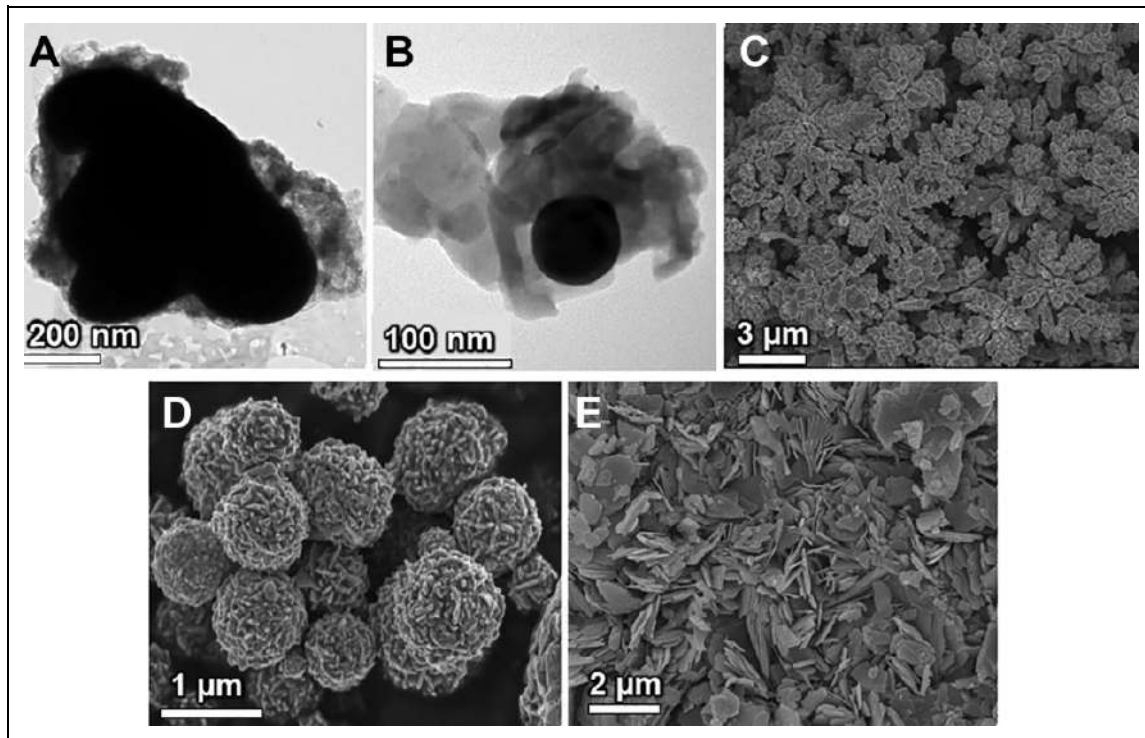


**Figure 5.** The unique physicochemical characteristic of each SB samples. (A) SB-A, (B) SB-B, (C) SB-C, (D) SB-D, and (E) SB-E. The morphology of any SB preparation did not match with others. Spherical gold nanoparticles were only observed in SB-B.

not contain arsenic. In the *Ayurved* process, Hg is commonly used in the manufacturing steps, but Hg was not found in any of the samples (they were below detection level). Absence of Hg (boiling temperature 356.73°C) can be explained. This could be due to the fact that in the *Ayurved* manufacturing process, since the temperature is >600°C, Hg should have completely evaporated during repetitive heat treatment.

The textual *Ayurved* process for *Bhasma* preparation includes numerous steps. Our experience in characterizing various *Bhasma* samples<sup>20,21</sup> and recent literature suggested that the control of the size and shape of *Bhasma* particles is challenging in the *Ayurved* process. Size distribution is always wide and particles are irregular in shape. In this study, we found that SB-A, SB-B and SB-E had irregular sizes and shapes. The size distribution in these 3 SB preparations was very wide (from nano to several micron sizes). In contrast, SB-C and SB-D samples had uniform-sized colloidal particles. Most interesting was the SB-D sample, which consisted of exact spherical and uniform gold particles. It can be surmised that SB-D was probably not manufactured by *Ayurvedic* process. Instead, direct synthesis, like a low-cost electrochemical approach, was supposed to be adopted for the preparation of SB-D sample. Guo and Wang<sup>22</sup> reported similar types of gold structures synthesized by the electrochemical method. Several other studies also showed SB-D alike gold particles,<sup>23-25</sup> synthesized by modern techniques. On the other hand, the uniform coral shaped micro-structure of SB-C also raised a similar suspicion, as this type of shape is unlikely to be observed in *Bhasma* samples known to be manufactured by traditional methods. Similarly, it is

possible that SB-C was not produced by the *Ayurved* process, but may have been directly synthesized because it had a coral-gold micro-structure that is very similar to what has been reported in the modern literature, in which it was chemically synthesized by a seed-mediated growth approach.<sup>26</sup>

A considerable amount of Arsenic was found in SB-A. In *Ayurved*, compounds of arsenic (*Somal-As<sub>2</sub>O<sub>3</sub>*, *Harital-As<sub>2</sub>S<sub>3</sub>*)<sup>27</sup> are being used in the management of some chronic diseases. The presence of arsenic in SB-A may have been intentional. It can be understood from the manufacturing process of SB-A, as *Somal* (As<sub>2</sub>O<sub>3</sub>) was used in the process (see Supplementary file 1). In the TGA analysis, approximately 10% weight loss up to 600°C inferred that substances associated with SB-A particles could have been arsenic oxides and carbonaceous material. Only SB-B had unique nano-sized, spherical gold particles that were entrapped in the crevices of bigger gold particles. The entrapment of spherical gold particles may occur during rigorous heat treatment steps. On the other hand, the red-colored SB-E was the sample with the lowest gold concentration. A substantial amount of iron oxide was present in it, which makes it brownish in appearance.

It is crucial to consider the pharmacokinetics (PK) of SB to investigate the bioavailability of gold. In contrast to small molecule drugs, most colloidal and nanoparticles exhibit complex pharmacokinetics *in vivo* due to a variety of physicochemical and biological factors. Particle uptake in the blood circulatory system can be affected by the morphology of particles. The efficacy of drugs is affected by its pharmacokinetics in the body. Here, in the rat model, we observed that the

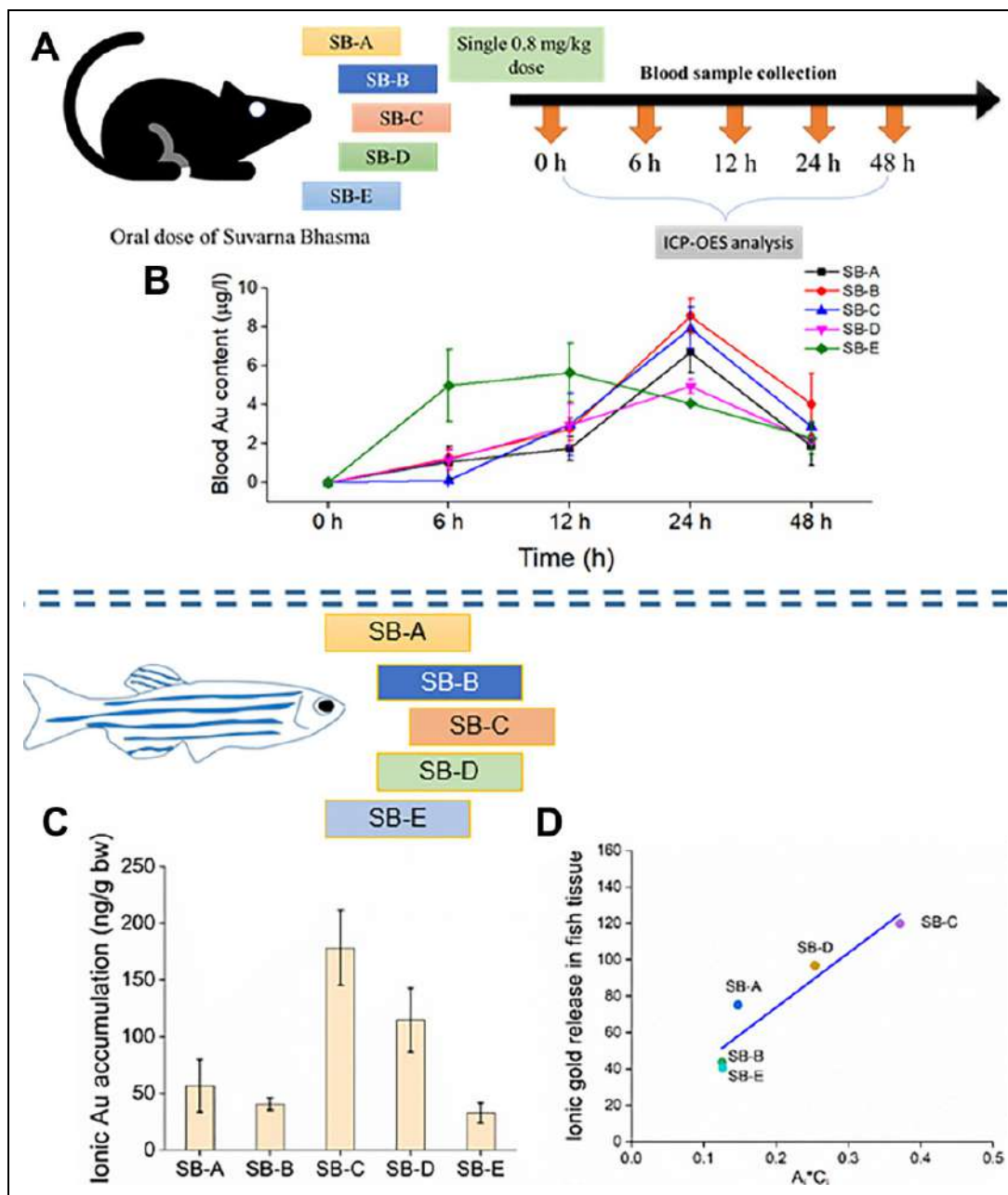


**Figure 6.** Pharmacokinetics of different SB preparations in rats and bioaccumulation of gold in zebrafish after oral administration. (A) Schematic diagram of PK experiment in rat, (B) time-dependent gold concentration in blood, (C) the released ionic Au from SB samples in zebrafish tissue. (D) The plot of ionic gold release in zebrafish from gold particles vs.  $A_1C_i$ . PK model shows that the  $C_{\max}$  was highest for SB-B at 24 h, whereas  $C_{\max}$  was lowest for SB-D ( $n = 4$  rats/group). Approximately 5.5-fold variation of ionic Au between SB-C and SB-E was observed. Ionic gold release data were linearly fitted with  $R^2 = 0.974$ , showing a strong correlation between the ionic gold in tissue to the physicochemical measurement.

pharmacokinetics of 5 SB preparations differed with respect to their maximum gold availability in the blood ( $C_{\max}$ ). This difference in  $C_{\max}$  could be due to the difference in their physicochemical properties.

Gold is an active element in SB for its desired therapeutic efficacy. There could be 2 possible mechanisms for the efficacy of SB: firstly, SB nano-sized particles can enter the cellular system and improve immune responses through an unknown

mechanism by binding with various proteins. Secondly, a very minute quantity of ionic gold can be released from gold particles in biological fluids, which may induce an adaptive mechanism in the biological system.

Gold can be transported through blood after an oral dose in 2 ways. A) as gold particle and B) ionic gold (Au). The solid gold particles after oral intake may remain intact in the gastrointestinal tract (GIT) due to its low solubility. However, gold particles

**Table 4.** Pharmacokinetic Parameters of 5 Different SB Preparations.

Parameter	SB-A	SB-B	SB-C	SB-D	SB-E
$\lambda_z$ (1/h)	0.065 ± 0.017 <sup>*d, e</sup>	0.035 ± 0.010	0.041 ± 0.006	0.030 ± 0.004 <sup>*a</sup>	0.028 ± 0.014 <sup>*a</sup>
$t_{1/2}$ (h)	13.73 ± 4.135	29.05 ± 10.62	17.89 ± 2.576	24.60 ± 3.601	54.23 ± 33.89
$T_{max}$ (h)	24.00 ± 0.000 <sup>*e</sup>	24.00 ± 0.000 <sup>*e</sup>	24.00 ± 0.000 <sup>*e</sup>	21.00 ± 3.000 <sup>*e</sup>	10.00 ± 2.000 <sup>*a, b, c, d</sup>
$C_{max}$ (µg/L)	6.705 ± 1.053	8.555 ± 0.926 <sup>*d</sup>	7.938 ± 1.086 <sup>*c</sup>	4.66 ± 0.464 <sup>*b, c</sup>	7.097 ± 1.071
$AUC_{0-t}$ (µg/L*h)	165.39 ± 34.26	234.59 ± 28.84 <sup>*d</sup>	204.93 ± 33.23	136.65 ± 17.66 <sup>*b</sup>	198.90 ± 14.64
$AUC_{0-inf\_obs}$ (µg/L*h)	213.76 ± 51.45	432.73 ± 96.61	279.09 ± 27.13	215.79 ± 15.79	443.61 ± 197.34
$AUMC_{0-inf\_obs}$ (µg/L*h <sup>2</sup> )	8273 ± 2671	28601 ± 12506	11365 ± 636	10540 ± 1310	535362 ± 44872
$MRT_{0-inf\_obs}$ (h)	36.308 ± 5.814	57.054 ± 15.62	41.714 ± 4.32	48.97 ± 5.453	79.91 ± 46.04
$Vz/F_{obs}$ (mg)/(µg/L/h)	0.074 ± 0.013	0.072 ± 0.013	0.078 ± 0.016	0.133 ± 0.018 <sup>*a, b, c</sup>	0.119 ± 0.030

Note: a, b, c, d and e denote significant difference against SB-A, SB-B, SB-C, SB-D and SB-E groups respectively. Fisher LSD was carried out with <sup>\*</sup>p < 0.05.

**Table 5.** Relation Between Ionic Gold Release and  $A_i \times C_i$ .

Sample	BET surface area ( $A_i$ )	Avg gold fraction ( $C_i$ ) in SBs (ICP-AES data)	$A_i \times C_i$	Ionic gold concentration (ng/g bw) from Figure 6C
SB-A	0.1736	0.85	0.1475	56.70
SB-B	0.1289	0.97	0.1250	40.79
SB-C	0.3825	0.96	0.3710	178.28
SB-D	0.2612	0.97	0.2533	114.72
SB-E	0.3608	0.35	0.1260	32.77

can release ionic Au in the biological medium from its surface. Especially in acidic medium, the dissolution of gold can increase. Except for SB-B, all other samples did not contain nano-gold particles. This could restrict the access of gold particles into the bloodstream *via* gastrointestinal adsorption. However, nano-sized particles are more vulnerable to cross the GIT, which was the reason for the highest  $C_{max}$  in rat blood in the case of SB-B. Whereas,  $C_{max}$  was second highest for SB-C, which can be explained by the highest ionic Au release.

Several physicochemical properties can affect the dissolution of ionic Au from SB particles such as surface area, gold % in SBs and surface coating. In this study, we found a strong linear correlation between ionic Au release and the product of surface area and the gold fraction ( $A_i C_i$ ) in SBs. Due to some fraction of SB-B in nanoparticles, the bioaccumulation of gold was maximum for SB-B in rat blood; however, ionic Au concentration in whole-body zebrafish tissue was lesser when compared to other SB samples. The reason behind this is the lower surface area of SB-B, which leads to lower ionic Au release from the surface. SB-C had coral-shaped structures with more numbers of crevices, which increased the surface area manifold as compared to other samples (BET surface area 0.38 m<sup>2</sup>/g). Hence, it showed the highest ionic Au concentration. SB-E had a high surface area (BET surface area 0.36 m<sup>2</sup>/g), although the ionic gold concentration in tissue was low due to the lower % of gold in SB-E as compared to the other 4 SBs. Thus, the reason for the varied biological presence and extent is well explained by their physicochemical differences.

Gold is not an essential element for the human body. Gold particles in the elemental form are non-toxic.<sup>28</sup> However, evidence shows that ionic Au can be released in acidic medium of

gold nanoparticles.<sup>29</sup> The released Au ions can increase reactive oxygen species in cellular systems. Furthermore, it elicited activation of caspase-3, which can mediate cell apoptosis *via* the intrinsic mitochondrial pathway.<sup>29</sup> Our study found differences in the accumulation of ionic gold in zebrafish tissue from various SB administration. The highest concentration of ionic gold was 178 ng/g body weight of zebrafish with a dose of 0.1 mg/g (the single dose was ~ 50 times higher than the therapeutic dose of SB in humans) of SB. The ionic Au accumulation from all the SB preparations should not result in any harmful effects as ionic gold is not toxic at low concentrations (LD<sub>50</sub> of ionic Au is about 430 mg/kg, which is equivalent to 430 µg/g in rat).<sup>30</sup>

This research is limited to the physicochemical properties and its concentration profile of gold (which is the main component) in animal models. Moreover, this study does not provide any light on the efficacy or toxicity of those 5 marketed *Suvarna Bhasma* sample. However, looking at the physicochemical variation, it is clear that the biological action of these 5 samples should be different from each other. Therefore, a comprehensive study of their efficacy and toxicity is required to compare their medicinal supremacy. Furthermore, the physicochemical factors that could be the main reason for the efficacy of *Suvarna Bhasma* were not explored in animal models. The accumulation of gold in individual tissues could have been provided more insight about its pharmacokinetics.

## Conclusion

This study investigated the differences in *Suvarna Bhasma* prepared by 5 different manufacturers with no morphological similarities between them. Two of these samples were

suspected not to be manufactured as per the claimed *Ayurved* textual procedure. We have demonstrated that the particle structure of the 5 SBs studied here are different from each other with different shapes and sizes, which in turn lead to differences in pharmacokinetic profiles in the rat models. Therefore, this study concludes that the physicochemical structure as well as biological responses of these 5 preparations, were not similar, and hence efficacy and safety of these SB preparations from different manufacturers may vary. Therefore, this study advocates stringent control over the manufacturing process and the quality of SB.

### Authors' Note

Conceptualization: Snehasis Biswas (SB), Mukesh Chawda (MC), Jayesh Bellare (JB). Methodology: SB, Kapil Thakur (KT), Ramacharya Gudi (RG) Project administration: MC, JB. Supervision: JB. Writing: original draft: SB. Writing, review and editing: SB, MC, KT, RG, and JB. Animal experiments were conducted according to the Committee for the Purpose of Control and Supervision of Experiments on Animals (CPCSEA) guideline (SDARF/CT/2019/04), India.

### Acknowledgments

The authors would like to thank SAIF-and IRCC-Indian Institute of Technology Bombay (IITB), for providing infrastructure and facilities.

### Declaration of Conflicting Interests

The author(s) declared the following potential conflicts of interest with respect to the research, authorship, and/or publication of this article: Three of the co-authors are from Shree Dhootapapeshwar Limited, which has also funded the study. The first and corresponding authors declare no conflict of interest.

### Funding

The author(s) disclosed receipt of the following financial support for the research, authorship, and/or publication of this article: This project was financially supported by Shree Dhootapapeshwar Limited (grant no DO/2018-SDLP001), Mumbai, India.

### ORCID iD

Jayesh Bellare, PhD  <https://orcid.org/0000-0002-6792-8327>

### Supplemental Material

Supplemental material for this article is available online.

### References

1. Andrikopoulos A, Economou L. International review of financial analysis editorial board interlocks in financial economics. *Int Rev Financ Anal*. 2015;37:51-62. doi:10.1016/j.irfa.2014.11.015
2. Pal C, Sahu CK, Haldar A. Bhasma : the ancient Indian nanomedicine. *J Adv Pharm Technol Res*. 2014;5(1):4-12. doi:10.4103/2231-4040.126980
3. Chen PC, Mwakwari SC, Oyelere AK. Gold nanoparticles : from nanomedicine to nanosensing. *Nanotechnol Sci Appl*. 2008;1:45-66.
4. Ghosh P, Han G, De M, Kim CK, Rotello VM. Gold nanoparticles in delivery applications. *Adv Drug Deliv Rev*. 2008;60(11):1307-1315. doi:10.1016/j.addr.2008.03.016
5. Patra CR, Bhattacharya R, Mukhopadhyay D, Mukherjee P. Fabrication of gold nanoparticles for targeted therapy in pancreatic cancer. *Adv Drug Deliv Rev*. 2010;62(3):346-361. doi:10.1016/j.addr.2009.11.007
6. Yadav KD, Chaudhary AK. Percentage of Swarna Bhasma in medicaments of Ayurveda to treat disorders of different origin. *Int J Green Pharm*. 2015;9(2):90-94. doi:10.4103/0973-8258.155053
7. Biswas S, Dhumal R, Selkar N, et al. Physicochemical characterization of Suvarna Bhasma, its toxicity profiling in rat and behavioural assessment in zebrafish model. *J Ethnopharmacol*. 2019;249:112388. doi:10.1016/j.jep.2019.112388
8. Mitra A, Chakraborty S, Auddy B, Tripathi P, Sen S, Saha AV. Evaluation of chemical constituents and free-radical scavenging activity of Swarna Bhasma (gold ash), an Ayurvedic drug. *J Ethnopharmacol*. 2002;80(2-3):147-153.
9. Beaudet D, Badilescu S, Kuruvinashetti K, et al. Comparative study on cellular entry of incinerated ancient gold particles (Swarna Bhasma) and chemically synthesized gold particles. *Sci Rep*. 2017;7(1):10678. doi:10.1038/s41598-017-10872-3
10. Brown CL, Bushell G, Whitehouse MW, et al. Nanogold-pharmaceutics traditional Indian medicine. *Gold Bull*. 2007;40(3):245-250.
11. Thakur K, Gudi R, Vahalia M, Shitut S, Nadkarni S. Preparation and characterization of Suvarna Bhasma Parada Marit. *J Pharmacopuncture*. 2017;20(1):36-44. doi:10.3831/KPI.2017.20.007
12. Liu X, Huang N, Li H, Jin Q, Ji J. Surface and size effects on cell interaction of gold nanoparticles with both phagocytic and non-phagocytic cells. *Langmuir*. 2013;29(29):9138-9148. doi:10.1021/la401556 k
13. Shah ZA, Gilani RA, Sharma P, Vohora SB. Attenuation of stress-elicited brain catecholamines, serotonin and plasma corticosterone levels by calcined gold preparations used in Indian system of medicine. *Basic Clin Pharmacol Toxicol*. 2005;96(6):469-474. doi:10.1111/j.1742-7843.2005.pto\_10.x
14. Woalder. Antibacterial activity and cytotoxicity of gold (I) and (III) ions and gold nanoparticles. *Physiol Behav*. 2015;4(1):139-148. doi:10.4172/2167-0501.1000199
15. Zhang Y, Huo M, Zhou J, Xie S. PKSolver: an add-in program for pharmacokinetic and pharmacodynamic data analysis in Microsoft Excel. *Comput Methods Programs Biomed*. 2010;99(3):306-314. doi:10.1016/j.cmpb.2010.01.007
16. Biswas S, Balodia N, Bellare J. Comparative neurotoxicity study of mercury-based inorganic compounds including Ayurvedic medicines Rasasindura and Kajjali in zebrafish model. *Neurotoxicol Teratol*. 2018;66:25-34. doi:10.1016/j.ntt.2018.01.007
17. Lee HB, Blaufox MD. Blood volume in the rat. *J Nucl Med*. 1985;25(1):72-76.
18. Saper R, Kales S, Paquin J. Heavy metal content of Ayurvedic herbal medicine products. *JAMA*. 2004;292(23):2868-2873. doi:10.1001/jama.292.23.2868
19. Yadav V, Makwana M, Kamble S, Qureshi F, Sarmalkar B. Different au-content in Swarna Bhasma preparations : evidence of

- lot-to-lot variations from different manufacturers. *Appl Sci Res.* 2012;3(6):3581-3586.
20. Aparna C, Ajit J, Shantaram K, Suresh AK, Jayesh B. Traditional method of Bhasma preparation generates stressed, polycrystalline, nano and submicron sized particles as revealed by physico-chemical studies of Suwarnamakshik Bhasma. *Adv Sci Lett.* 2014; 20(5-6):1211-1218. doi:10.1166/asl.2014.5490
  21. Bhowmick TK, Suresh AK, Kane SG, Joshi AC, Bellare JR. Physicochemical characterization of an Indian traditional medicine, Jasada Bhasma: detection of nanoparticles containing non-stoichiometric zinc oxide. *J Nanoparticle Res.* 2009;11(3): 655-664. doi:10.1007/s11051-008-9414-z
  22. Guo S, Wang E. Templateless, surfactantless, simple electrochemical route to rapid synthesis of diameter-controlled 3D flowerlike gold microstructure with "clean" surface. *Chem Commun.* 2007;(30):3163-3165. doi:10.1039/b705630c. Epub 2007 May 25.
  23. Muthurasu A, Yong H. Facile electrochemical synthesis of three dimensional flowerlike gold microstructure for electrochemical oxidation of hydrogen peroxide. *Electrochim Acta.* 2018;283: 1425-1431. doi:10.1016/j.electacta.2018.07.092
  24. Wang X, Huang P, Li M, et al. Hierarchically assembled Au microspheres and sea urchin-like architectures : formation mechanism and SERS study. *Nanoscale.* 2012;4(24):7766-7772. doi:10.1039/c2nr32405a. Epub 2012 Nov 8.
  25. Lu S, You T, Gao Y, Yang N, Zhang C, Yin P. Rapid fabrication of three-dimensional flower-like gold microstructures on flexible substrate for SERS applications. *Spectrochim Acta A Mol Biomol Spectrosc.* 2019;212:371-379. doi:10.1016/j.saa.2019.01.018
  26. Darienzo RE, Karius K, Obla N, Chang C, Mironava T. Synthesis of coral-shaped gold nanoparticles for SERS sensing applications. *Mater Res Express.* 2018;5(9):095003. doi:10.1088/2053-1591/aad48d
  27. Palbag S, Gautam DNS. Arsenic in the management of leukemia: an Ayurvedic perspective. *J Ayurvedic Herb Med.* 2017;3(3): 159-162.
  28. Shukla R, Bansal V, Chaudhary M, Basu A, Bhonde RR, Sastry M. Biocompatibility of gold nanoparticles and their endocytotic fate inside the cellular compartment : a microscopic overview. *Langmuir.* 2005;21(25):10644-10654. doi:10.1021/la0513712
  29. Sabella S, Carney RP, Brunetti V, et al. A general mechanism for intracellular toxicity of metal-containing nanoparticles. *Nanoscale.* 2014;6(12):7052-7061. doi:10.1039/c4nr01234 h
  30. Egorova KS, Ananikov VP. Toxicity of metal compounds: knowledge and myths. *Organometallics.* 2017;36(21):4071-4090. doi: 10.1021/acs.organomet.7b00605